

Spectral engineering of integrated photonic filters using mode splitting in silicon nanowire integrated standing-wave resonators

David J. Moss

^a Centre for Micro-Photonics, Swinburne University of Technology, Hawthorn, 3122, Australia

* Electronic mail: djoss@swin.edu.au

ABSTRACT

Mode splitting induced by coherent optical mode interference in coupled resonant cavities is a key phenomenon in photonic resonators that can lead to powerful and versatile filtering functions, in close analogy to electromagnetically-induced-transparency, Autler-Townes splitting, Fano resonances, and dark states. It can not only break the dependence between quality factor, free spectral range, and physical cavity length, but can also lead to group delay response and mode interactions that are useful for enhancing light-material interaction and dispersion engineering in nonlinear optics. In this work, we investigate mode splitting in standing-wave (SW) resonators implemented by cascaded Sagnac loop reflectors (CSLRs) and demonstrate its use for engineering the spectral profile of integrated photonic filters. By changing the reflectivity of the Sagnac loop reflectors (SLRs) and the phase shifts along the connecting waveguides, we tailor mode splitting in the CSLR resonators to achieve a wide range of filter shapes for diverse applications including enhanced light trapping, flat-top filtering, Q factor enhancement, and signal reshaping. We present the theoretical designs and compare the performance of CSLR resonators with three, four, and eight SLRs fabricated in silicon-on-insulator nanowires. We achieve high performance and versatile filter shapes via diverse mode splitting that agree well with theory. The experimental results confirm the effectiveness of our approach towards realizing integrated multi-functional SW filters for flexible spectral engineering.

Keywords: Integrated photonics, mode splitting, standing-wave resonator

1. INTRODUCTION

Along with the development of advanced micro/nano fabrication technologies, integrated photonic resonators with compact footprints, mass-producibility, high scalability, and versatile filtering properties have been a subject of great interest and become key building blocks for signal modulation, buffering, switching, and processing in optical communication systems [1–3]. Similar to atomic resonance splitting caused by quantum interference between excitation pathways in multi-level atomic systems [4], mode splitting induced by coherent interference between optical modes in coupled resonant cavities is a fundamental phenomenon in integrated photonic resonators, which can lead to many meaningful filtering spectra such as optical analogues of electromagnetically-induced-transparency (EIT), Fano resonances, Autler-Townes splitting (ATS), and dark states [5–7]. Another attractive merit of mode splitting is that it can break the fundamental dependence between quality factor, free spectra range (FSR), and physical cavity length [8–10], which is useful for the implementation of integrated photonic resonators with reduced device footprints and power consumptions. Moreover, the group delay responses and mode interactions generated by mode splitting can also be utilized for enhanced light-material interaction and dispersion engineering in nonlinear optics [11–14].

Generally speaking, photonic resonators can be classified into two categories, namely, travelling-wave (TW) resonators and standing-wave (SW) resonators [15, 16]. The microring resonator (MRR) is a typical example of a TW resonator, while the photonic crystal cavity, distributed feedback cavity, and Fabry-Perot cavity are representatives of SW resonators. To implement integrated photonic resonators with mode splitting, considerable works have been reported [5, 17–22]. Most of these works are based on coupled TW resonators, and in some recent works there are also several device structures constructed by both TW and SW resonators [20, 21]. Considering that the physical cavity length of a TW resonator is almost twice longer as compared with a SW resonator with the same FSR [23], integrated resonators implemented by SW resonators are more attractive in terms of reduced device footprints. In addition, unlike nearly uniform field distribution in TW resonators, there are spacially-dependent field distributions in SW resonators, which are crucial for efficient excitation of laser emission and nonlinear optical effects [16, 24].

In this paper, we investigate mode splitting in integrated photonic resonators implemented by SW resonators. The SW resonators are realized based on multiple cascaded Sagnac loop reflectors (SLRs). The basic idea of photonic resonators formed by cascaded SLRs (we termed as CSLR resonators) was proposed in Ref. [25] and experimental demonstrations of CSLR resonators with two SLRs were reported in Refs. [23, 26]. For CSLR resonators with more than two SLRs, mode splitting occurs due to coherent interference between the FP cavities formed by different SLRs. Here we provide detailed theory of mode splitting in CSLR resonators for spectral engineering and experimental demonstration of CSLR resonators with up to eight SLRs. By changing the reflectivity of the SLRs and the phase shifts along the connecting waveguides, mode splitting in the CSLR resonator can be tailored for diverse applications such as enhanced light trapping, flat-top filtering, Q factor enhancement, and signal reshaping. We present a theoretical analysis for the operation principle, and fabricate the designed CSLR resonators on a silicon-on-insulator (SOI) platform. For the fabricated devices with different numbers of the SLRs, versatile filter shapes that corresponds to diverse mode splitting conditions are experimentally achieved. The experimental results agree well with theory and confirm the effectiveness of the CSLR resonator as a multi-functional SW filter for flexible spectral engineering.

2. DEVICE STRUCTURE AND OPERATION PRINCIPLE

Figure 1 illustrates the schematic configuration of the integrated CSLR resonator. It consists of N SLRs ($SLR_1, SLR_2, \dots, SLR_N$) formed by a self-coupled nanowire waveguide loop. In the CSLR resonator, each SLR performs as a reflection/transmission element and contributes to the overall transmission spectra from port IN to port OUT in Fig. 1. Therefore, the cascaded SLRs with a periodic loop lattice show similar transmission characteristics to that of photonic crystals [25, 27]. The two adjacent SLRs together with the connecting waveguide form a FP cavity, thereby N cascaded SLRs can also be regarded as $N-1$ cascaded FP cavities ($FPC_1, FPC_2, \dots, FPC_{N-1}$), similar to Bragg gratings [16, 28, 29]. To study the CSLR resonator based on the scattering matrix method (SMM) [30–32], we define the waveguide and coupler parameters of the CSLR resonator in Table I. The large dynamic range in engineering the transmittance and reflectivity of individual SLRs via changing t_i or κ_i makes the CSLR resonator more flexible for spectral engineering as compared with Bragg gratings. On the other hand, the transmission spectra of the CSLR resonators can also be tailored by changing φ_i ($i = 1, 2, \dots, N-1$), i.e., the phase shifts along the connecting waveguides. The freedom in designing t_i ($i = 1, 2, \dots, N$) and φ_i ($i = 1, 2, \dots, N-1$) is the basis for flexible spectral engineering based on the CSLR resonators, which can lead to versatile applications.

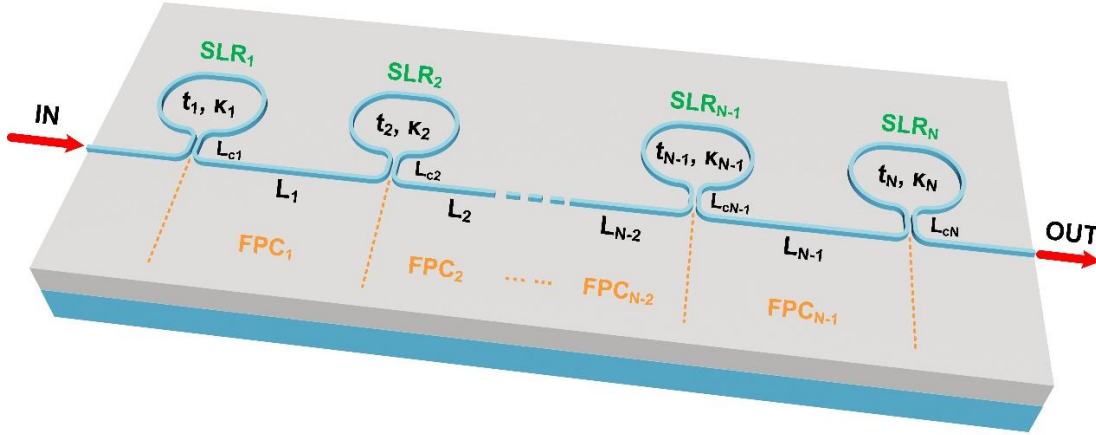


FIG. 1. Schematic configuration of integrated CSLR resonator made up of N cascaded SLRs ($SLR_1, SLR_2, \dots, SLR_N$). FPC_i ($i = 1, 2, \dots, N-1$) are the FP cavities formed by SLR_i and SLR_{i+1} , respectively. The definitions of t_i ($i = 1, 2, \dots, N$), κ_i ($i = 1, 2, \dots, N$), L_{ci} ($i = 1, 2, \dots, N$), and L_i ($i = 1, 2, \dots, N-1$) are given in Table I.

CSLR resonators with two SLRs ($N = 2$) can be regarded as single FP cavities without mode splitting [23, 26]. Here, we start from the CSLR resonators with three SLRs ($N = 3$). The calculated power transmission spectra and group delay spectra of the CSLR resonators with three SLRs ($N = 3$) are depicted in Fig. 2. The structural parameters are chosen as follows: $L_{s1} = L_{s2} = L_{s3} = 129.66 \mu\text{m}$, and $L_1 = L_2 = 100 \mu\text{m}$. For single-mode silicon photonic nanowire waveguides with

TABLE I. Definitions of waveguide and coupler parameters of the CSLR resonator

Waveguide	Length	Transmission factor ^a	Phase shift ^b
waveguide connecting SLR _{<i>i</i>} to SLR _{<i>i</i>+1} (<i>i</i> = 1, 2, ..., <i>N</i> -1)	L_i	a_i	φ_i
Sagnac loops in SLR _{<i>i</i>} (<i>i</i> = 1, 2, ..., <i>N</i>)	L_{si}	a_{si}	φ_{si}
Coupler	Coupling length ^c	Field transmission coefficient ^d	Field cross-coupling coefficient ^d
couplers in SLR _{<i>i</i>} (<i>i</i> = 1, 2, ..., <i>N</i>)	L_{ci}	t_i	κ_i

^a $a_i = \exp(-\alpha L_i/2)$, $a_{si} = \exp(-\alpha L_{si}/2)$, α is the power propagation loss factor.

^b $\varphi_i = 2\pi n_g L_i/\lambda$, $\varphi_{si} = 2\pi n_g L_{si}/\lambda$, n_g is the group index and λ is the wavelength.

^c L_{ci} (*i* = 1, 2, ..., *N*) are the straight coupling lengths shown in Fig.1. They are included in L_i .

^d In our calculation, we assume $t_i^2 + \kappa_i^2 = 1$ for lossless coupling in all the directional couplers.

a cross-section of 500 nm × 260 nm, we also assume that the waveguide group index of the transverse electric (TE) mode is $n_g = 4.3350$ and the power propagation loss factor is $\alpha = 55 \text{ m}^{-1}$ (2.4 dB/cm) based on our previously fabricated devices. The same n_g and α are also employed for the calculations of other transmission and group delay spectra in this section. It is clear that different degrees of mode splitting can be achieved by varying t_2 . As t_2 decreases (i.e., the coupling strength increases), the spectral range between the two adjacent resonant peaks decreases until the split peaks finally merge into one. By further decreasing t_2 , the Q factor, extinction ratio, and group delay of the combined single resonance increases, together with an increase in the insertion loss. In particular, when $t_2 = 0.77$, a band-pass Butterworth filter with a flat-top filter shape can be realized, which is desirable for signal filtering in optical communications systems. On the other hand, when $t_2 = 0.742$, the CSLR resonator exhibits a flat-top group delay spectrum, which can be used as a Bessel filter for optical buffering.

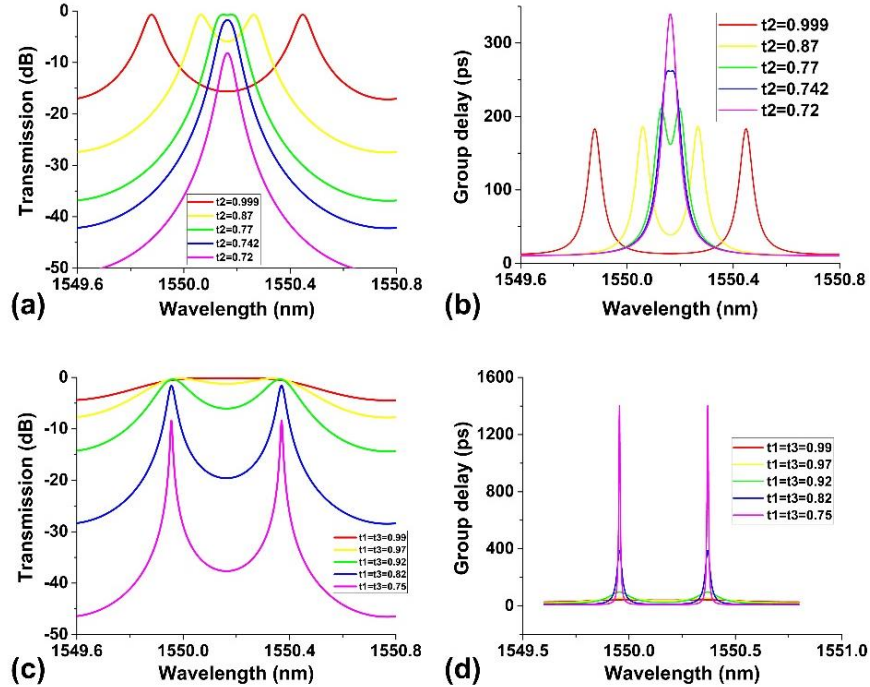


FIG. 2. (a) Calculated power transmission spectra of the CSLR resonator ($N = 3$) for various t_2 when $t_1 = t_3 = 0.87$. (b) Calculated group delay spectra of the CSLR resonator ($N = 3$) for various t_2 when $t_1 = t_3 = 0.87$. (c) Calculated power transmission spectra of the CSLR resonator ($N = 3$) for various $t_1 = t_3$ when $t_2 = 0.97$. (d) Calculated group delay spectra of the CSLR resonator ($N = 3$) for various $t_1 = t_3$ when $t_2 = 0.97$.

Figure 3(a) shows the calculated power transmission spectra of the CSLR resonators with different numbers of SLRs (N). It can be seen that as N increases, the number of split resonances within one FSR also increases. For a CSLR resonator consisting of N SLRs, the maximum number of split resonances within one FSR is $N-1$. In Fig. 3(b), we plot the calculated power transmission spectra of the CSLR resonator ($N = 8$) for different $t_1 = t_2 = \dots = t_8$. As t_i ($i = 1, 2, \dots, 8$) increases (i.e., the coupling strengths decrease), the bandwidth of the passband also increases, together with a decrease in insertion loss. In principle, the bandwidth of the passband is limited by the FSR of the CSLR resonator. The filter in Figs. 3(c) and (d) is designed for enhanced light trapping by introducing an additional $\pi/2$ phase shift along the centre FPC (i.e., L_4 for $N = 8$), which is similar to enhancing light trapping in photonic crystals by introducing defects [25]. With enhanced light trapping, there are increased time delays and enhanced light-matter interactions, which are useful in nonlinear optics and laser excitation [27]. In Fig. 3(c), one can see that there are central transmission peaks induced by an additional phase shift along L_4 , which correspond to a group delay 2.1 times higher than that of the CSLR resonator without the additional phase shift in Fig. 3(d). This group delay can be increased further by using more cascaded SLRs. The filter in Fig. 3(e) is an 8th-order Butterworth filter with a flat-top filter shape. Figure 3(f) shows the designed optical filter with multiple transmission peaks in the spectrum. Each transmission peak has a high extinction ratio over 10 dB.

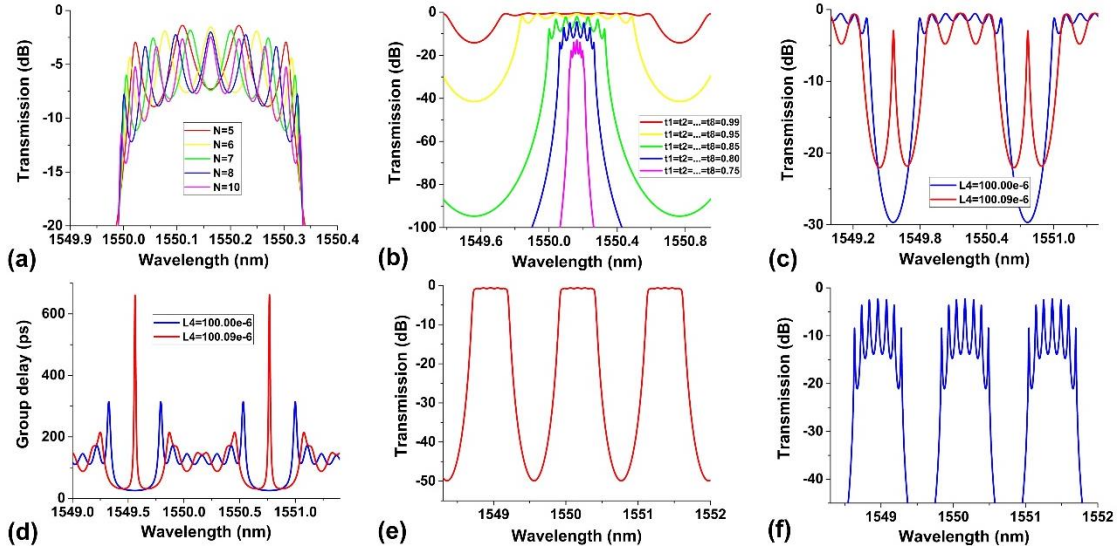


FIG. 3. (a) Calculated power transmission spectra of the CSLR resonator for various N when $t_1 = t_2 = \dots = t_N = 0.85$. (b) Calculated power transmission spectra of the CSLR resonator ($N = 8$) for different $t_1 = t_2 = \dots = t_8$. (c) Calculated power transmission spectra of the CSLR resonator ($N = 8$) for enhanced light trapping. (d) Calculated group delay spectra of the CSLR resonator ($N = 8$) in (c). (e) Calculated power transmission spectra of 8th-order Butterworth filter based on the CSLR resonator ($N = 8$). (f) Calculated power transmission spectra of the CSLR resonator ($N = 8$) with multiple transmission peaks.

3. DEVICE FABRICATION AND CHARACTERIZATION

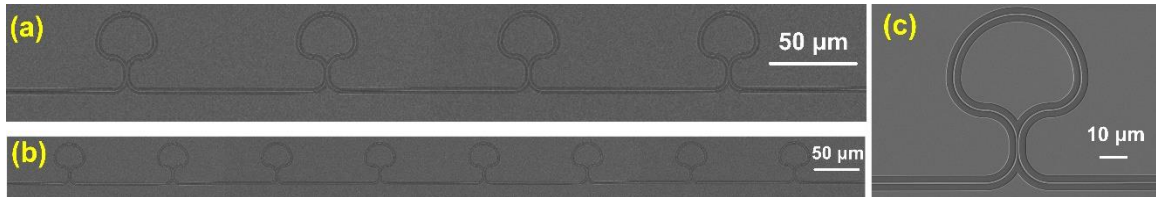


FIG. 4. (a) Micrograph for one of the fabricated CSLR resonators with four SLRs. (b) Micrograph for one of the fabricated CSLR resonators with eight SLRs. (c) Zoom-in micrograph for the SLR.

We fabricated a series of CSLR filters based on the above designs on an SOI wafer. The micrographs for the fabricated devices with four and eight SLRs are shown in Figs. 4(a) and (b), respectively. A zoom-in micrograph for the SLR is shown in Fig. 4(c). The normalized transmission spectra for the fabricated CSLR resonators with three SLRs ($N = 3$) are shown in Figs. 5(a) and (b) by the blue solid curves. The normalized spectra are then fit by the red dashed curves calculated based on the SMM. In Fig. 5(a), various mode splitting spectra of the fabricated devices with different L_{c2} are obtained,

which are consistent with the theory in Fig. 2(a). The measured spectra of the fabricated devices with different $L_{c1} = L_{c3}$ in Fig. 5(b) also agree well with the theory in Fig. 2(c).

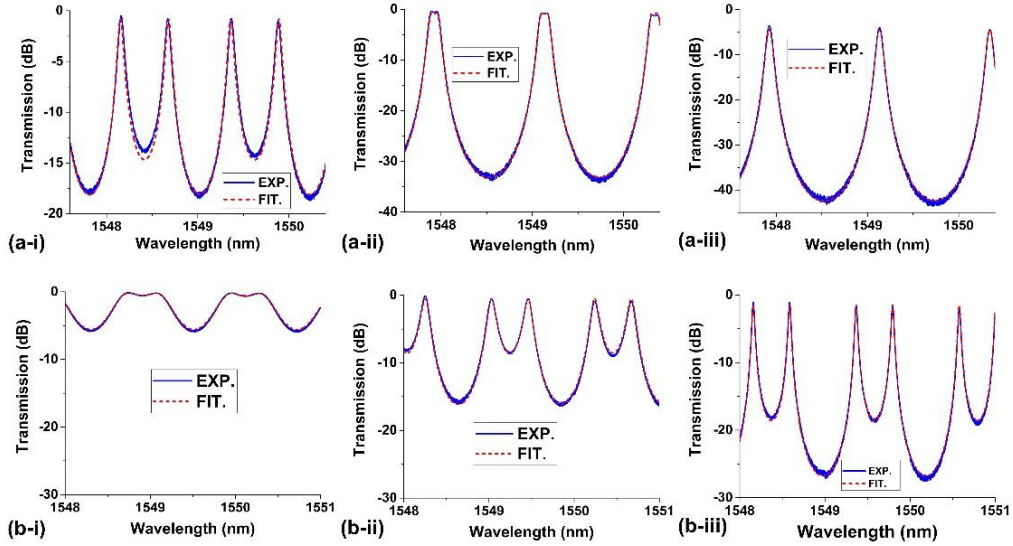


FIG. 5. (a) Measured (solid curve) and fit (dashed curve) transmission spectra of three fabricated CSLR resonators ($N = 3$) with different L_{c2} . (b) Measured (solid curve) and fit (dashed curve) transmission spectra of three fabricated CSLR resonators ($N = 3$) with different $L_{c1} = L_{c3}$.

The measured and fit transmission spectra of the fabricated CSLR resonators with four SLRs ($N = 4$) are shown in Fig. 6(a). Figures 6(b) – (d) show the measured and fit transmission spectra of the fabricated CSLR resonators with eight SLRs ($N = 8$). The device in Fig. 6(b) is designed for enhanced light trapping, and the measured transmission spectrum is similar to the calculated spectrum in Fig. 3(c). The measured filter shape in Fig. 6(b) exhibit a slight asymmetry, and this is because the additional phase shift along L_4 is not exactly $\pi/2$. By introducing thermo-optic micro-heaters or carrier-injection electrodes [26] along L_4 to tune the phase shift, the symmetry of the filter shape can be improved further. The device in Fig. 6(c) was designed to perform as an 8th-order Butterworth filter with a flat-top filter shape. As can be seen, the passband is almost flat, which is close to the calculated spectrum in Fig. 3(e). The slight unevenness of the top can be attributed to the discrepancies between the designed and practical coupling coefficients. Figure 6(d) shows the measured transmission spectrum with multiple resonant peaks. The minimum extinction ratio of the transmission peaks is ~ 7.8 dB, which is slightly lower than that in Fig. 3(f). This is mainly because the waveguide propagation loss of the fabricated devices ($\alpha = 64 \text{ m}^{-1}$) is slightly higher than we assumed in the calculation ($\alpha = 55 \text{ m}^{-1}$). By further reducing the propagation loss [33–36], as has been achieved in doped silica glass platforms such as Hydex, [37–85] higher extinction ratios of the split resonances can be obtained. These circuits with their high performance and low footprint will be highly useful for quantum optical integrated circuits [86–98] as well as for nonlinear optics involving 2D materials such as graphene oxide. [99–116]

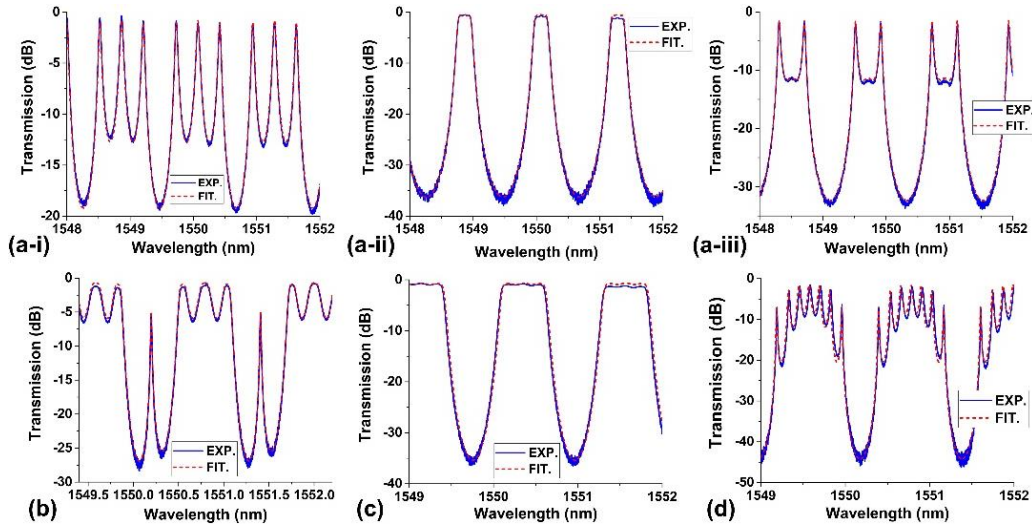


FIG. 6. (a) Measured (solid curve) and fit (dashed curve) transmission spectra of three fabricated CSLR resonators ($N = 4$) with different L_{ci} ($i = 1, 2, 3, 4$). (b) Measured (solid curve) and fit (dashed curve) transmission spectra of a fabricated CSLR resonator ($N = 8$) for enhanced light trapping. (c) Measured (solid curve) and fit (dashed curve) transmission spectra of a fabricated CSLR resonator ($N = 8$) with flat-top filter shape. (d) Measured (solid curve) and fit (dashed curve) transmission spectra of a fabricated CSLR resonator ($N = 8$) with multiple split resonances.

4. CONCLUSION

In summary, we investigate mode splitting in standing-wave resonators formed by cascaded Sagnac loop reflectors (CSLRs) and demonstrate its use for engineering the spectral profile of integrated photonic filters. By changing the reflectivity of the Sagnac loop reflectors (SLRs) and the phase shifts along the connecting waveguides, we tailor the mode splitting to achieve a wide range of filter shapes for diverse applications including enhanced light trapping, Q factor enhancement, and signal reshaping. We present theoretical designs and experimentally demonstrate versatile filter shapes corresponding to diverse mode splitting conditions that agree well with theory.

Conflict of Interest

The authors declare that there are no conflicts of interest.

REFERENCES

- [1] S. Q. Feng, T. Lei, H. Chen, H. Cai, X. S. Luo, and A. W. Poon, "Silicon photonics: from a microresonator perspective," *Laser & Photonics Reviews*, vol. 6, no. 2, pp. 145-177, Mar, 2012.
- [2] J. Wu, P. Cao, X. Hu, T. Wang, M. Xu, X. Jiang, F. Li, L. Zhou, and Y. Su, "Nested Configuration of Silicon Microring Resonator With Multiple Coupling Regimes," *IEEE Photonics Technology Letters*, vol. 25, no. 6, pp. 580-583, 2013.
- [3] J. Wu, J. Peng, B. Liu, T. Pan, H. Zhou, J. Mao, Y. Yang, C. Qiu, and Y. Su, "Passive silicon photonic devices for microwave photonic signal processing," *Optics Communications*, vol. 373, pp. 44-52, 2016.
- [4] M. Fleischhauer, A. Imamoglu, and J. P. Marangos, "Electromagnetically induced transparency: Optics in coherent media," *Reviews of Modern Physics*, vol. 77, no. 2, pp. 633-673, Apr, 2005.
- [5] L. Verslegers, Z. Yu, Z. Ruan, P. B. Catrysse, and S. Fan, "From electromagnetically induced transparency to superscattering with a single structure: a coupled-mode theory for doubly resonant structures," *Phys Rev Lett*, vol. 108, no. 8, pp. 083902, Feb 24, 2012.
- [6] M. F. Limonov, M. V. Rybin, A. N. Poddubny, and Y. S. Kivshar, "Fano resonances in photonics," *Nature Photonics*, vol. 11, no. 9, pp. 543-554, 2017.
- [7] B. Peng, S. K. Ozdemir, W. Chen, F. Nori, and L. Yang, "What is and what is not electromagnetically induced transparency in whispering-gallery microcavities," *Nat Commun*, vol. 5, pp. 5082, Oct 24, 2014.
- [8] J. Wu, P. Cao, T. Pan, Y. Yang, C. Qiu, C. Tremblay, and Y. Su, "Compact on-chip 1×2 wavelength selective switch based on silicon microring resonator with nested pairs of subrings," *Photonics Research*, vol. 3, no. 1, pp. 9, 2014.

- [9] S. Lai, Z. Xu, B. Liu, and J. Wu, "Compact silicon photonic interleaver based on a self-coupled optical waveguide," *Appl Opt*, vol. 55, no. 27, pp. 7550-5, Sep 20, 2016.
- [10] M. C. Souza, G. F. Rezende, L. A. Barea, A. A. von Zuben, G. S. Wiederhecker, and N. C. Frateschi, "Spectral engineering with coupled microcavities: active control of resonant mode-splitting," *Opt Lett*, vol. 40, no. 14, pp. 3332-5, Jul 15, 2015.
- [11] Y. Yang, J. Wu, X. Xu, Y. Liang, S. T. Chu, B. E. Little, R. Morandotti, B. Jia, and D. J. Moss, "Invited Article: Enhanced four-wave mixing in waveguides integrated with graphene oxide," *APL Photonics*, vol. 3, no. 12, pp. 120803, 2018.
- [12] J. Leuthold, C. Koos, and W. Freude, "Nonlinear silicon photonics," *Nature Photonics*, vol. 4, no. 8, pp. 535-544, 2010.
- [13] X. Sun, C. Qiu, J. Wu, H. Zhou, T. Pan, J. Mao, X. Yin, R. Liu, W. Gao, Z. Fang, and Y. Su, "Broadband photodetection in a microfiber-graphene device," *Opt Express*, vol. 23, no. 19, pp. 25209-16, Sep 21, 2015.
- [14] J. Wu, X. Xu, T. G. Nguyen, S. T. Chu, B. E. Little, R. Morandotti, A. Mitchell, and D. J. Moss, "RF Photonics: An Optical Microcombs' Perspective," *IEEE Journal of Selected Topics in Quantum Electronics*, vol. 24, no. 4, pp. 1-20, 2018.
- [15] Q. Li, T. Wang, Y. K. Su, M. Yan, and M. Qiu, "Coupled mode theory analysis of mode-splitting in coupled cavity system," *Optics Express*, vol. 18, no. 8, pp. 8367-8382, Apr 12, 2010.
- [16] L. Lu, F. Li, M. Xu, T. Wang, J. Wu, L. Zhou, and Y. Su, "Mode-Selective Hybrid Plasmonic Bragg Grating Reflector," *IEEE Photonics Technology Letters*, vol. 24, no. 19, pp. 1765-1767, 2012.
- [17] X. Mu, W. Jiayang, W. Tao, H. Xiaofeng, J. Xinhong, and S. Yikai, "Push-Pull Optical Nonreciprocal Transmission in Cascaded Silicon Microring Resonators," *IEEE Photonics Journal*, vol. 5, no. 1, pp. 2200307-2200307, 2013.
- [18] L. Zhang, J. Wu, X. Yin, X. Sun, P. Cao, X. Jiang, and Y. Su, "A High-Speed Second-Order Photonic Differentiator Based on Two-Stage Silicon Self-Coupled Optical Waveguide," *IEEE Photonics Journal*, vol. 6, no. 2, pp. 1-5, 2014.
- [19] L. A. M. Barea, F. Vallini, G. F. M. de Rezende, and N. C. Frateschi, "Spectral Engineering With CMOS Compatible SOI Photonic Molecules," *IEEE Photonics Journal*, vol. 5, no. 6, pp. 2202717-2202717, 2013.
- [20] A. Li, and W. Bogaerts, "Tunable electromagnetically induced transparency in integrated silicon photonics circuit," *Opt Express*, vol. 25, no. 25, pp. 31688-31695, Dec 11, 2017.
- [21] S. Zheng, Z. S. Ruan, S. Q. Gao, Y. Long, S. M. Li, M. B. He, N. Zhou, J. Du, L. Shen, X. L. Cai, and J. Wang, "Compact tunable electromagnetically induced transparency and Fano resonance on silicon platform," *Optics Express*, vol. 25, no. 21, pp. 25655-25662, Oct 16, 2017.
- [22] J. Wu, X. Jiang, T. Pan, P. Cao, L. Zhang, X. Hu, and Y. Su, "Non-blocking 2×2 switching unit based on nested silicon microring resonators with high extinction ratios and low crosstalks," *Chinese Science Bulletin*, vol. 59, no. 22, pp. 2702-2708, 2014.
- [23] X. M. Sun, L. J. Zhou, J. Y. Xie, Z. Zou, L. J. Lu, H. K. Zhu, X. W. Li, and J. P. Chen, "Tunable silicon Fabry-Perot comb filters formed by Sagnac loop mirrors," *Optics Letters*, vol. 38, no. 4, pp. 567-569, Feb 15, 2013.
- [24] F. Li, X. Sun, J. Wu, X. Hu, L. Zhou, and Y. Su, "Efficient Fiber-to-Slot-Waveguide Grating Couplers Based on a Double-Strip Waveguide," *IEEE Photonics Technology Letters*, vol. 25, no. 23, pp. 2377-2380, 2013.
- [25] J. F. Song, L. W. Luo, X. S. Luo, H. F. Zhou, X. G. Tu, L. X. Jia, Q. Fang, and G. Q. Lo, "Loop coupled resonator optical waveguides," *Optics Express*, vol. 22, no. 20, pp. 24202-24216, Oct 6, 2014.
- [26] X. Jiang, J. Wu, Y. Yang, T. Pan, J. Mao, B. Liu, R. Liu, Y. Zhang, C. Qiu, C. Tremblay, and Y. Su, "Wavelength and bandwidth-tunable silicon comb filter based on Sagnac loop mirrors with Mach-Zehnder interferometer couplers," *Opt Express*, vol. 24, no. 3, pp. 2183-8, Feb 8, 2016.
- [27] T. Pan, C. Qiu, J. Wu, X. Jiang, B. Liu, Y. Yang, H. Zhou, R. Soref, and Y. Su, "Analysis of an electro-optic modulator based on a graphene-silicon hybrid 1D photonic crystal nanobeam cavity," *Opt Express*, vol. 23, no. 18, pp. 23357-64, Sep 7, 2015.
- [28] X. Wang, Y. Wang, J. Flueckiger, R. Bojko, A. Liu, A. Reid, J. Pond, N. A. F. Jaeger, and L. Chrostowski, "Precise control of the coupling coefficient through destructive interference in silicon waveguide Bragg gratings," *Optics Letters*, vol. 39, no. 19, pp. 5519-5522, Oct 1, 2014.
- [29] Y. Zhang, Y. He, J. Wu, X. Jiang, R. Liu, C. Qiu, X. Jiang, J. Yang, C. Tremblay, and Y. Su, "High-extinction-ratio silicon polarization beam splitter with tolerance to waveguide width and coupling length variations," *Opt Express*, vol. 24, no. 6, pp. 6586-93, Mar 21, 2016.
- [30] J. Wu, T. Moein, X. Xu, G. Ren, A. Mitchell, and D. J. Moss, "Micro-ring resonator quality factor enhancement via an integrated Fabry-Perot cavity," *APL Photonics*, vol. 2, no. 5, pp. 056103, 2017.
- [31] J. Wu, T. Moein, X. Xu, and D. J. Moss, "Advanced photonic filters based on cascaded Sagnac loop reflector resonators in silicon-on-insulator nanowires," *APL Photonics*, vol. 3, no. 4, pp. 046102, 2018.
- [32] J. Wu, B. Liu, J. Peng, J. Mao, X. Jiang, C. Qiu, C. Tremblay, and Y. Su, "On-Chip Tunable Second-Order Differential-Equation Solver Based on a Silicon Photonic Mode-Split Microresonator," *Journal of Lightwave Technology*, vol. 33, no. 17, pp. 3542-3549, 2015.
- [33] X. Xu, J. Wu, T. G. Nguyen, S. T. Chu, B. E. Little, R. Morandotti, A. Mitchell, and D. J. Moss, "Broadband RF Channelizer Based on an Integrated Optical Frequency Kerr Comb Source," *Journal of Lightwave Technology*, vol. 36, no. 19, pp. 4519-4526, 2018.
- [34] X. Xu, J. Wu, T. G. Nguyen, T. Moein, S. T. Chu, B. E. Little, R. Morandotti, A. Mitchell, and D. J. Moss, "Photonic microwave true time delays for phased array antennas using a 49 GHz FSR integrated optical micro-comb source [Invited]," *Photonics Research*, vol. 6, no. 5, pp. B30, 2018.

- [35] X. Xu, J. Wu, T. G. Nguyen, M. Shoeiby, S. T. Chu, B. E. Little, R. Morandotti, A. Mitchell, and D. J. Moss, "Advanced RF and microwave functions based on an integrated optical frequency comb source," *Opt Express*, vol. 26, no. 3, pp. 2569-2583, Feb 5, 2018.
- [36] X. Xu, *et al.*, "Orthogonally polarized RF optical single sideband generation and dual-channel equalization based on an integrated microring resonator," *Journal of Lightwave Technology*, vol. 36, no. 20, pp. 4808-4818. 2018.
37. X. Xu, M. Tan, J. Wu, R. Morandotti, A. Mitchell, and D. J. Moss, "Microcomb-based photonic RF signal processing", *IEEE Photonics Technology Letters*, vol. 31 no. 23 1854-1857, 2019.
38. M. Tan *et al.*, "Orthogonally polarized Photonic Radio Frequency single sideband generation with integrated micro-ring resonators", *IOP Journal of Semiconductors*, Vol. **42** (4), 041305 (2021). DOI: [10.1088/1674-4926/42/4/041305](https://doi.org/10.1088/1674-4926/42/4/041305).
39. Xu, *et al.*, "Advanced adaptive photonic RF filters with 80 taps based on an integrated optical micro-comb source," *Journal of Lightwave Technology*, vol. 37, no. 4, pp. 1288-1295 (2019).
40. X. Xu, *et al.*, "Broadband microwave frequency conversion based on an integrated optical micro-comb source", *Journal of Lightwave Technology*, vol. 38 no. 2, pp. 332-338, 2020.
41. M. Tan, *et al.*, "Photonic RF and microwave filters based on 49GHz and 200GHz Kerr microcombs", *Optics Comm.* vol. 465,125563, Feb. 22. 2020.
42. X. Xu, *et al.*, "Broadband photonic RF channelizer with 90 channels based on a soliton crystal microcomb", *Journal of Lightwave Technology*, Vol. 38, no. 18, pp. 5116 - 5121, 2020. doi: [10.1109/JLT.2020.2997699](https://doi.org/10.1109/JLT.2020.2997699).
43. X. Xu, *et al.*, "Photonic RF and microwave integrator with soliton crystal microcombs", *IEEE Transactions on Circuits and Systems II: Express Briefs*, vol. 67, no. 12, pp. 3582-3586, 2020. DOI:[10.1109/TCSII.2020.2995682](https://doi.org/10.1109/TCSII.2020.2995682).
44. X. Xu, *et al.*, "High performance RF filters via bandwidth scaling with Kerr micro-combs," *APL Photonics*, vol. 4 (2) 026102. 2019.
45. M. Tan, *et al.*, "Microwave and RF photonic fractional Hilbert transformer based on a 50 GHz Kerr micro-comb", *Journal of Lightwave Technology*, vol. 37, no. 24, pp. 6097 – 6104, 2019.
46. M. Tan, *et al.*, "RF and microwave fractional differentiator based on photonics", *IEEE Transactions on Circuits and Systems: Express Briefs*, vol. 67, no.11, pp. 2767-2771, 2020. DOI:[10.1109/TCSII.2020.2965158](https://doi.org/10.1109/TCSII.2020.2965158).
47. M. Tan, *et al.*, "Photonic RF arbitrary waveform generator based on a soliton crystal micro-comb source", *Journal of Lightwave Technology*, vol. 38, no. 22, pp. 6221-6226 (2020). DOI: [10.1109/JLT.2020.3009655](https://doi.org/10.1109/JLT.2020.3009655).
48. M. Tan, X. Xu, J. Wu, R. Morandotti, A. Mitchell, and D. J. Moss, "RF and microwave high bandwidth signal processing based on Kerr Micro-combs", *Advances in Physics X*, VOL. 6, NO. 1, 1838946 (2021). DOI:[10.1080/23746149.2020.1838946](https://doi.org/10.1080/23746149.2020.1838946).
49. M. Tan, X. Xu, J. Wu, B. Corcoran, A. Boes, T. G. Nguyen, S. T. Chu, B. E. Little, R. Morandotti, A. Lowery, A. Mitchell, and D. J. Moss, "'Highly Versatile Broadband RF Photonic Fractional Hilbert Transformer Based on a Kerr Soliton Crystal Microcomb", *Journal of Lightwave Technology* vol. 39 (24) 7581-7587 (2021).
50. Wu, J. *et al.* RF Photonics: An Optical Microcombs' Perspective. *IEEE Journal of Selected Topics in Quantum Electronics* Vol. **24**, 6101020, 1-20 (2018).
51. T. G. Nguyen *et al.*, "Integrated frequency comb source-based Hilbert transformer for wideband microwave photonic phase analysis," *Opt. Express*, vol. 23, no. 17, pp. 22087-22097, Aug. 2015.
52. X. Xu, J. Wu, M. Shoeiby, T. G. Nguyen, S. T. Chu, B. E. Little, R. Morandotti, A. Mitchell, and D. J. Moss, "Reconfigurable broadband microwave photonic intensity differentiator based on an integrated optical frequency comb source," *APL Photonics*, vol. 2, no. 9, 096104, Sep. 2017.
53. X. Xu, *et al.*, "Continuously tunable orthogonally polarized RF optical single sideband generator based on micro-ring resonators," *Journal of Optics*, vol. 20, no. 11, 115701. 2018.
54. X. Xu, *et al.*, "Photonic RF phase-encoded signal generation with a microcomb source", *J. Lightwave Technology*, vol. 38, no. 7, 1722-1727, 2020.
55. B. Corcoran, *et al.*, "Ultra-dense optical data transmission over standard fiber with a single chip source", *Nature Communications*, vol. 11, Article:2568, 2020.
56. X. Xu *et al.*, "Photonic perceptron based on a Kerr microcomb for scalable high speed optical neural networks", *Laser and Photonics Reviews*, vol. 14, no. 8, 2000070 (2020). DOI: [10.1002/lpor.202000070](https://doi.org/10.1002/lpor.202000070).
57. X. Xu, *et al.*, "11 TOPs photonic convolutional accelerator for optical neural networks", *Nature* **589**, 44-51 (2021).
58. Xingyuan Xu, Weiwei Han, Mengxi Tan, Yang Sun, Yang Li, Jiayang Wu, Roberto Morandotti, Fellow IEEE, Arnan Mitchell, Senior Member IEEE, Kun Xu, and David J. Moss, Fellow IEEE Mengxi Tan, Xingyuan Xu, Jiayang Wu, Roberto Morandotti, Arnan Mitchell, and David J. Moss, "Neuromorphic computing based on wavelength-division multiplexing", *28 Early Access IEEE Journal of Selected Topics in Quantum Electronics Special Issue on Optical Computing*. DOI:[10.1109/JSTQE.2022.3203159](https://doi.org/10.1109/JSTQE.2022.3203159).
59. Yang Sun, Jiayang Wu, Mengxi Tan, Xingyuan Xu, Yang Li, Roberto Morandotti, Arnan Mitchell, and David Moss, "Applications of optical micro-combs", *Advances in Optics and Photonics* (2022).
60. Yunping Bai, Xingyuan Xu,1, Mengxi Tan, Yang Sun, Yang Li, Jiayang Wu, Roberto Morandotti, Arnan Mitchell, Kun Xu, and David J. Moss, "Photonic multiplexing techniques for neuromorphic computing", *Nanophotonics* (2022).

61. Chawaphon Prayoonyong, Andreas Boes, Xingyuan Xu, Mengxi Tan, Sai T. Chu, Brent E. Little, Roberto Morandotti, Arnan Mitchell, David J. Moss, and Bill Corcoran, "Frequency comb distillation for optical superchannel transmission", *Journal of Lightwave Technology* 39 (23) 7383-7392 (2021). DOI: 10.1109/JLT.2021.3116614.
62. Mengxi Tan, Xingyuan Xu, Jiayang Wu, Bill Corcoran, Andreas Boes, Thach G. Nguyen, Sai T. Chu, Brent E. Little, Roberto Morandotti, Arnan Mitchell, and David J. Moss, "Integral order photonic RF signal processors based on a soliton crystal microcomb source", *IOP Journal of Optics* 23 (11) 125701 (2021). <https://doi.org/10.1088/2040-8986/ac2eab>
63. A. Pasquazi, et al., "Sub-picosecond phase-sensitive optical pulse characterization on a chip", *Nature Photonics*, vol. 5, no. 10, pp. 618-623 (2011).
64. Bao, C., et al., Direct soliton generation in microresonators, *Opt. Lett.*, **42**, 2519 (2017).
65. M.Ferrera et al., "CMOS compatible integrated all-optical RF spectrum analyzer", *Optics Express*, vol. 22, no. 18, 21488 - 21498 (2014).
66. M. Kues, et al., "Passively modelocked laser with an ultra-narrow spectral width", *Nature Photonics*, vol. 11, no. 3, pp. 159, 2017.
67. L. Razzari, et al., "CMOS-compatible integrated optical hyper-parametric oscillator," *Nature Photonics*, vol. 4, no. 1, pp. 41-45, 2010.
68. M. Ferrera, et al., "Low-power continuous-wave nonlinear optics in doped silica glass integrated waveguide structures," *Nature Photonics*, vol. 2, no. 12, pp. 737-740, 2008.
69. M.Ferrera et al. "On-Chip ultra-fast 1st and 2nd order CMOS compatible all-optical integration", *Opt. Express*, vol. 19, (23)pp. 23153-23161 (2011).
70. D. Duchesne, M. Peccianti, M. R. E. Lamont, et al., "Supercontinuum generation in a high index doped silica glass spiral waveguide," *Optics Express*, vol. 18, no. 2, pp. 923-930, 2010.
71. H Bao, L Olivieri, M Rowley, ST Chu, BE Little, R Morandotti, DJ Moss, ... "Turing patterns in a fiber laser with a nested microresonator: Robust and controllable microcomb generation", *Physical Review Research* **2** (2), 023395 (2020).
72. M. Ferrera, et al., "On-chip CMOS-compatible all-optical integrator", *Nature Communications*, vol. 1, Article 29, 2010.
73. A. Pasquazi, et al., "All-optical wavelength conversion in an integrated ring resonator," *Optics Express*, vol. 18, no. 4, pp. 3858-3863, 2010.
74. A.Pasquazi, Y. Park, J. Azana, et al., "Efficient wavelength conversion and net parametric gain via Four Wave Mixing in a high index doped silica waveguide," *Optics Express*, vol. 18, no. 8, pp. 7634-7641, 2010.
75. M. Peccianti, M. Ferrera, L. Razzari, et al., "Subpicosecond optical pulse compression via an integrated nonlinear chirper," *Optics Express*, vol. 18, no. 8, pp. 7625-7633, 2010.
76. Little, B. E. et al., "Very high-order microring resonator filters for WDM applications", *IEEE Photonics Technol. Lett.* **16**, 2263-2265 (2004).
77. M. Ferrera et al., "Low Power CW Parametric Mixing in a Low Dispersion High Index Doped Silica Glass Micro-Ring Resonator with Q-factor > 1 Million", *Optics Express*, vol.17, no. 16, pp. 14098-14103 (2009).
78. M. Peccianti, et al., "Demonstration of an ultrafast nonlinear microcavity modelocked laser", *Nature Communications*, vol. 3, pp. 765, 2012.
79. A.Pasquazi, et al., "Self-locked optical parametric oscillation in a CMOS compatible microring resonator: a route to robust optical frequency comb generation on a chip," *Optics Express*, vol. 21, no. 11, pp. 13333-13341, 2013.
80. A.Pasquazi, et al., "Stable, dual mode, high repetition rate mode-locked laser based on a microring resonator," *Optics Express*, vol. 20, no. 24, pp. 27355-27362, 2012.
81. Pasquazi, A. et al. Micro-combs: a novel generation of optical sources. *Physics Reports* **729**, 1-81 (2018).
82. Moss, D. J. et al., "New CMOS-compatible platforms based on silicon nitride and Hydex for nonlinear optics", *Nature photonics* **7**, 597 (2013).
83. H. Bao, et al., Laser cavity-soliton microcombs, *Nature Photonics*, vol. 13, no. 6, pp. 384-389, Jun. 2019.
84. Antonio Cutrona, Maxwell Rowley, Debayan Das, Luana Olivieri, Luke Peters, Sai T. Chu, Brent L. Little, Roberto Morandotti, David J. Moss, Juan Sebastian Toterogongora, Marco Peccianti, Alessia Pasquazi, "High Conversion Efficiency in Laser Cavity-Soliton Microcombs", *Optics Express* Vol. 30, Issue 22, pp. 39816-39825 (2022). <https://doi.org/10.1364/OE.470376>.
85. M.Rowley, P.Hazard, A.Cutrona, H.Bao, S.Chu, B.Little, R.Morandotti, D. J. Moss, G. Oppo, J. Gongora, M. Peccianti and A. Pasquazi, "Self-emergence of robust solitons in a micro-cavity", *Nature* **608** (7922) 303-309 (2022).
86. Kues, M. et al. Quantum optical microcombs. *Nature Photonics* **13**, (3) 170-179 (2019). doi:10.1038/s41566-019-0363-0

87. C.Reimer, L. Caspani, M. Clerici, et al., "Integrated frequency comb source of heralded single photons," *Optics Express*, vol. 22, no. 6, pp. 6535-6546, 2014.
88. C.Reimer, et al., "Cross-polarized photon-pair generation and bi-chromatically pumped optical parametric oscillation on a chip", *Nature Communications*, vol. 6, Article 8236, 2015. DOI: 10.1038/ncomms9236.
89. L. Caspani, C. Reimer, M. Kues, et al., "Multifrequency sources of quantum correlated photon pairs on-chip: a path toward integrated Quantum Frequency Combs," *Nanophotonics*, vol. 5, no. 2, pp. 351-362, 2016.
90. C. Reimer et al., "Generation of multiphoton entangled quantum states by means of integrated frequency combs," *Science*, vol. 351, no. 6278, pp. 1176-1180, 2016.
91. M. Kues, et al., "On-chip generation of high-dimensional entangled quantum states and their coherent control", *Nature*, vol. 546, no. 7660, pp. 622-626, 2017.
92. P. Roztock et al., "Practical system for the generation of pulsed quantum frequency combs," *Optics Express*, vol. 25, no. 16, pp. 18940-18949, 2017.
93. Y. Zhang, et al., "Induced photon correlations through superposition of two four-wave mixing processes in integrated cavities", *Laser and Photonics Reviews*, vol. 14, no. 7, pp. 2000128, 2020. DOI: 10.1002/lpor.202000128
94. C. Reimer, et al., "High-dimensional one-way quantum processing implemented on d-level cluster states", *Nature Physics*, vol. 15, no.2, pp. 148-153, 2019.
95. P.Roztock et al., "Complex quantum state generation and coherent control based on integrated frequency combs", *Journal of Lightwave Technology* **37** (2) 338-347 (2019).
96. S. Sciarra et al., "Generation and Processing of Complex Photon States with Quantum Frequency Combs", *IEEE Photonics Technology Letters* **31** (23) 1862-1865 (2019). DOI: 10.1109/LPT.2019.2944564.
97. Stefania Sciarra, Piotr Roztock, Bennet Fisher, Christian Reimer, Luis Romero Cortez, William J. Munro, David J. Moss, Alfonso C. Cino, Lucia Caspani, Michael Kues, J. Azana, and Roberto Morandotti, "Scalable and effective multilevel entangled photon states: A promising tool to boost quantum technologies", *Nanophotonics* **10** (18), 4447-4465 (2021). DOI:10.1515/nanoph-2021-0510.
98. L. Caspani, C. Reimer, M. Kues, et al., "Multifrequency sources of quantum correlated photon pairs on-chip: a path toward integrated Quantum Frequency Combs," *Nanophotonics*, vol. 5, no. 2, pp. 351-362, 2016.
99. Yuning Zhang, Jiayang Wu, Yang Qu, Yunyi Yang, Linnan Jia, Baohua Jia, and David J. Moss, "Enhanced supercontinuum generated in SiN waveguides coated with GO films", *Invited Paper, Advanced Material Technologies due Nov 15 (2022)*.
100. Yuning Zhang, Jiayang Wu, Linnan Jia, Yang Qu, Baohua Jia, and David J. Moss, "Graphene oxide for nonlinear integrated photonics", *Laser and Photonics Reviews* (IF=13.3).
101. Jiayang Wu, H.Lin, D. J. Moss, T.K. Loh, Baohua Jia, "Graphene oxide: new opportunities for electronics, photonics, and optoelectronics", *Nature Reviews Chemistry* (2022).
102. Yang Qu, Jiayang Wu, Yuning Zhang, Yunyi Yang, Linnan Jia, Baohua Jia, and David J. Moss, "Photo thermal tuning in GO-coated integrated waveguides", *Micromachines (MDPI) special issue on Nonlinear Optics with 2D Materials* **13** 1194 (2022). doi.org/10.3390/mi13081194
103. Yuning Zhang, Jiayang Wu, Yunyi Yang, Yang Qu, Houssein El Dirani, Romain Crochemore, Corrado Sciancalepore, Pierre Demongodin, Christian Grillet, Christelle Monat, Baohua Jia, and David J. Moss, "Enhanced self-phase modulation in silicon nitride waveguides integrated with 2D graphene oxide films", *Invited Paper, IEEE Journal of Selected Topics in Quantum Electronics (JSTQE) Special Issue on Integrated Nonlinear Optics* **28** Early Access (2022). DOI: 10.1109/JSTQE.2022.3177385
104. Yuning Zhang, Jiayang Wu, Yunyi Yang, Yang Qu, Linnan Jia, Baohua Jia, and David J. Moss, "Enhanced spectral broadening of femtosecond optical pulses in silicon nanowires integrated with 2D graphene oxide films", *Micromachines (MDPI) special issue on Nonlinear Optics with 2D Materials (Jiayang guest editor) Micromachines* **13** 756 (2022). DOI:10.3390/mi13050756 (2022).
105. Linnan Jia, Jiayang Wu, Yuning Zhang, Yang Qu, Baohua Jia, Zhigang Chen, and David J. Moss, "Fabrication Technologies for the On-Chip Integration of 2D Materials", *Small: Methods* **6**, 2101435 (2022). DOI:10.1002/smt.202101435.
106. Yuning Zhang, Jiayang Wu, Yang Qu, Linnan Jia, Baohua Jia, and David J. Moss, "Design and optimization of four-wave mixing in microring resonators integrated with 2D graphene oxide films", *Journal of Lightwave Technology* **39** (20) 6553-6562 (2021). DOI:10.1109/JLT.2021.3101292. Print ISSN: 0733-8724, Online ISSN: 1558-2213 (2021).
107. Yuning Zhang, Jiayang Wu, Yang Qu, Linnan Jia, Baohua Jia, and David J. Moss, "Optimizing the Kerr nonlinear optical performance of silicon waveguides integrated with 2D graphene oxide films", *Journal of Lightwave Technology* **39** (14) 4671-4683 (2021). DOI: 10.1109/JLT.2021.3069733.

108. Yang Qu, Jiayang Wu, Yuning Zhang, Yao Liang, Baohua Jia, and David J. Moss, "Analysis of four-wave mixing in silicon nitride waveguides integrated with 2D layered graphene oxide films", *Journal of Lightwave Technology* 39 (9) 2902-2910 (2021). DOI: 10.1109/JLT.2021.3059721.
109. Jiayang Wu, Linnan Jia, Yuning Zhang, Yang Qu, Baohua Jia, and David J. Moss, "Graphene oxide: versatile films for flat optics to nonlinear photonic chips", *Advanced Materials* 33 (3) 2006415, pp.1-29 (2021). DOI:10.1002/adma.202006415.
110. Y. Qu, J. Wu, Y. Zhang, L. Jia, Y. Yang, X. Xu, S. T. Chu, B. E. Little, R. Morandotti, B. Jia, and D. J. Moss, "Graphene oxide for enhanced optical nonlinear performance in CMOS compatible integrated devices", Paper No. 11688-30, PW21O-OE109-36, 2D Photonic Materials and Devices IV, SPIE Photonics West, San Francisco CA March 6-11 (2021). doi.org/10.1117/12.2583978
111. Yang Qu, Jiayang Wu, Yunyi Yang, Yuning Zhang, Yao Liang, Houssein El Dirani, Romain Crochemore, Pierre Demongodin, Corrado Sciancalepore, Christian Grillet, Christelle Monat, Baohua Jia, and David J. Moss, "Enhanced nonlinear four-wave mixing in silicon nitride waveguides integrated with 2D layered graphene oxide films", *Advanced Optical Materials* 8 (21) 2001048 (2020). DOI: 10.1002/adom.202001048. arXiv:2006.14944.
112. Yuning Zhang, Yang Qu, Jiayang Wu, Linnan Jia, Yunyi Yang, Xingyuan Xu, Baohua Jia, and David J. Moss, "Enhanced Kerr nonlinearity and nonlinear figure of merit in silicon nanowires integrated with 2D graphene oxide films", *ACS Applied Materials and Interfaces* 12 (29) 33094- 33103 June 29 (2020). DOI:10.1021/acsami.0c07852
113. Jiayang Wu, Yunyi Yang, Yang Qu, Yuning Zhang, Linnan Jia, Xingyuan Xu, Sai T. Chu, Brent E. Little, Roberto Morandotti, Baohua Jia,* and David J. Moss*, "Enhanced nonlinear four-wave mixing in microring resonators integrated with layered graphene oxide films", *Small* 16 (16) 1906563 April 23 (2020). DOI: 10.1002/smll.201906563
114. Jiayang Wu, Yunyi Yang, Yang Qu, Xingyuan Xu, Yao Liang, Sai T. Chu, Brent E. Little, Roberto Morandotti, Baohua Jia, and David J. Moss, "Graphene oxide waveguide polarizers and polarization selective micro-ring resonators", Paper 11282-29, SPIE Photonics West, San Francisco, CA, 4 - 7 February (2020). doi: 10.1117/12.2544584
115. Jiayang Wu, Yunyi Yang, Yang Qu, Xingyuan Xu, Yao Liang, Sai T. Chu, Brent E. Little, Roberto Morandotti, Baohua Jia, and David J. Moss, "Graphene oxide waveguide polarizers and polarization selective micro-ring resonators", *Laser and Photonics Reviews* 13 (9) 1900056 (2019). DOI:10.1002/lpor.201900056.
116. Yunyi Yang, Jiayang Wu, Xingyuan Xu, Sai T. Chu, Brent E. Little, Roberto Morandotti, Baohua Jia, and David J. Moss, "Enhanced four-wave mixing in graphene oxide coated waveguides", *Applied Physics Letters (APL) Photonics* 3 120803 (2018); doi: 10.1063/1.5045509.